https://doi.org/10.17163/abyaups.92.705

Validation of the Tensile Test of A36 Steel Through Finite Element Method and Experimental Data

Isaac Simbaña
Grupo de Investigación en Ingeniería Mecánica y Pedagogía de la Carrera de Electromecánica (GIIMPCEM), Instituto Superior Universitario Sucre, Ecuador
Orcid: https://orcid.org/0000-0002-3324-3071

David Saquinga
Grupo de Investigación en Ingeniería Mecánica y Pedagogía de la Carrera de Electromecánica (GIIMPCEM), Instituto Superior Universitario Sucre, Ecuador
Orcid: https://orcid.org/0000-0001-8353-1621

Marco Macías
Grupo de Investigación en Ingeniería Mecánica y Pedagogía de la Carrera de Electromecánica (GIIMPCEM), Instituto Superior Universitario Sucre, Ecuador
Orcid: https://orcid.org/0009-0004-5386-4790

Leonidas Ramírez
Grupo de Investigación en Ingeniería, Productividad y Simulación Industrial (GIIPSI), Universidad Politécnica Salesiana, Ecuador
Orcid: https://orcid.org/0000-0003-2569-2974

Introduction

Structural steel, manufactured under the standards set by the American Society for Testing and Materials (ASTM) A36, finds widespread use in construction and structural engineering. Its versatility stems from its availability in various profiles and sheets, making it essential in the construction of buildings, industrial facilities, suspension bridge cables, and reinforcements (ASTM International, 2019). A36 structural steel is the primary material choice for building and bridge construction due to its ubiquity and reliability. Its low carbon content and absence of alloying elements are often linked to AISI 1018 steel due to its similar chemical composition (Márquez-Herrera et al., 2022). Moreover, its use facilitates compatibility with complementary materials at a reduced cost for finishing. However, drawbacks include the need for costly maintenance, as the material is susceptible to corrosion and necessitates periodic painting. Exposure to high temperatures can compromise its

structural integrity, while its profiles are prone to deformation with any torsion or movement (Rahangmetan et al., 2020).

The mechanical properties of a material encompass its inherent strength and resilience when subjected to external forces. In essence, they define a material's capacity to transmit and endure forces or deformations (Rodríguez et al., 2022). These properties are essential during the designing phase, as materials intended for engineering applications must exhibit sufficient mechanical strength to withstand various loads. This strength is quantified as stress, representing the relationship between the applied force and the cross-sectional area (Fajardo et al., 2019). Stress manifests as tension, compression, or stretching within a body subjected to an axial load, serving as a key indicator of how materials respond to external forces, potentially leading to deformation or fracture (Ramos-Quintero et al., 2022).

To ascertain the characteristics and properties of materials, researchers conduct experiments commonly referred to as material tests.

Gunter et al. (2021) describe these tests as laboratory experiments aimed at determining attributes such as stiffness, wear resistance, thermal or electrical conductivity, acidity, corrosion resistance, density, sound transmission, ductility, and impact resistance. A prevalent approach involves destructive testing, where methods are used to induce damage or breakage to the sample under analysis. This helps in comprehending and forecasting how the material will respond to various physical stresses, essentially assessing its capacity to withstand such pressures (Prakash-Pasupulla et al., 2022). In destructive tests, the material cannot be reused, as these procedures often push the material's physical properties to their limits, sometimes surpassing them until failure occurs. This process aids in identifying the material's behavior in extreme conditions.

Material tests serve various purposes such as material testing and enhancement, defect detection and evaluation in the metal industry, failure analysis, and fundamental research on material strength. Tensile testing stands as a key mechanical method used to determine the characteristic values of materials. Throughout the tensile test, the force and elongation of the specimen are measured (Liao et al., 2020). The applied tensile force tends to stretch the material from both ends, allowing for the determination of its strength, until failure occurs. As the load reaches its maximum, a concentration of deformations occurs in the central zone, leading to necking and a reduction in cross-sectional area. As noted by Dhoska (2019), the test becomes unstable, and the resisted load gradually decreases over time.

Calderón et al. (2021) scrutinized the experimental outcomes concerning the tensile strength and hardness of A36 structural steel. Their experimental framework encompassed accounting for temperature fluctuations during the welding process, which triggers alterations in the steel's internal structure, thereby delineating a correlation between stren-

gth and hardness. The specimens exhibited an augmentation in their maximum stress tolerance, reaching up to 440 MPa. Additionally, it was affirmed that the surface hardness diminishes in the fusion zone owing to temperature variations, which affect these properties. In contrast, Serrano and Albán (2022) assessed the mechanical properties of welded joints employing A36 structural steel. The study was conducted experimentally and also using ANSYS software for simulations, with a relative error of less than 10 % between both analyses. They determined that the maximum stress attained was 468.68 MPa in flat specimens with an 8 mm thickness. These values are significantly influenced by the welding process used to obtain the specimens, indicating that thicker welds will increase the cross-sectional area, enabling them to support a greater load and resulting in higher stress.

The finite element method (FEM) is a numerical technique used to approximate the deformation of mechanical elements by defining various boundary and initial conditions, including movement constraints and the application of external forces, along with their directions (Vantyghem et al., 2020). This method entails breaking down the geometry of an element into small finite-sized elements with simple geometries and finite dimensions. Within each of these small elements, simple interpolation functions are established to correlate the displacements of individual points, known as nodes, within the finite element to the displacement of a series of characteristic points within it. This process simplifies differential equations into algebraic equations that establish the relationship between the forces at the nodes and their displacements within each finite element (Arroba et al., 2021). By solving these algebraic equations for the finite elements composing the element and combining them, a system of equations is formulated for the original element. This approach provides an approximate solution for the displacement of each node in the problem, and subsequently for any point, utilizing the defined interpolation functions (González et al., 2020).

Larsen and Thorstensen (2020) highlight that this method originated in the 1 950s and has since found widespread use in both industry and research, enabling the analysis of an object's behavior without necessitating its physical construction. García-Garrino et al. (2021) conducted studies on processing challenges in Solid Mechanics, particularly focusing on large elastoplastic deformations using computational numerical simulation. The dominant tetrahedral technique has been deemed the most effective for mesh generation due to its versatility in adapting to various geometries. Moreover, adhering to the dimensions specified for specimens in different standards, simulation results have yielded the desired values for mechanical properties. It is advisable to gradually update work methodologies, such as integrating virtual machines (VMs) to allow the modification of one or more variables to obtain results for the dependent variables.

Computer-aided design (CAD) leverages computer systems as supportive tools across all processes involved in designing and manufacturing diverse products. Rigorous quality tests have been conducted, validating that the implemented components function correctly and meet specified requirements across various applications (Falivene et al., 2019). The primary utility entails utilizing computers to facilitate the creation, modification, analysis, or optimization of designs. In 3D modeling, it is notably straightforward to analyze surfaces and solidsBarenghi et al. (2019) suggest that CAD expedites task completion. CAD software is geared towards streamlining mechanical modeling in both 2D and 3D, offering diverse options for generating precise extractions, plans, and exchange files (Zhou et al., 2020).

On the other hand, computer-aided engineering (CAE), has evolved in response to the demands imposed by ongoing technological progress. Through CAE, a wide array of analyses can be performed, extending beyond structures or fluids to encompass thermodynamic processes, and acoustic and electromagnetic phenomena, among others. CAE software stands as a cornerstone tool in engineering, particularly in stress simulation and safety factor analysis. Wei et al. (2021) point out the availability of various CAE software applications for designing, analyzing, and simulating parts using finite element methods. These applications offer options for 3D modeling or importing geometries from CAD software, facilitating the transition to the preparation stage by generating a mesh and ensuring the discretized element is ready for FEM analysis. The outcomes of these simulations are instrumental in assessing the potential failure of specific components under defined load conditions and determining the requisite safety factors to be integrated into the design. This ensures stability during operation, mitigating the risk of mechanical failures induced by excessive loading forces beyond the parameters expected in typical usage scenarios (Alshoaibi and Ali-Fageehi, 2022).

Research conducted by Erazo-Arteaga (2022) delved into the design, manufacturing, and computer-aided engineering (CAD/CAM/CAE) of product development in Latin America. Over the past decade, there has been significant evolution, particularly evident in the enhancements in vehicle, machinery, and general industrial supplies design and production. Notable progress has also been made in the development of prosthetics and medical equipment. There is a growing trend towards digital manufacturing development, which integrates these tools into automated facilities, adhering to the philosophy of global thinking and local manufacturing. One of the primary advantages of employing these computer-assisted techniques is cost reduction, starting with reduced time dedicated to the design, optimization, and manufacturing of various elements. Furthermore, the elimination of the need to construct prototypes for performance evaluation conserves essential resour-

ces, as this type of software enables the prediction of object behavior under specified conditions. Berselli et al. (2020) introduced CAD/CAE-based learning tools for use in higher education, particularly in engineering disciplines. Software optimization has led to improved result accuracy and a more user-friendly interface, contributing to the increasing application of these technologies across diverse industries.

Li et al. (2020) conducted experimental and numerical studies on the tensile strength of concrete specimens reinforced with structural steel fibers. The steel improved tensile deformation, mitigating the brittleness of structural elements. The relative error between the experimental procedure and numerical results was below 15 %. However, mathematical modeling enables the approximation of responses under various conditions, including impact and fatigue. Serrano-Aguiar et al. (2021) investigated the effect of cracks in welded joints of A36 structural steel under tension through computational numerical simulation. A qualitative analysis was performed using SolidWorks and ANSYS software, considering round A36 structural steel pipes ranging from 100 to 500 mm in diameter, available in the market. Upon applying an axial stress of 250 MPa to prevent permanent deformation of the pipes, it was found that cracks acted as stress concentrators, with a relative error of 1.46 % between the experimental process and simulations for equivalent stress, reaching 648.5 MPa before fracture. Therefore, the authors concluded that the safety factor should be increased by 0.35 units to meet the requirements.

This study aims to validate obtained stress results through computational numerical analysis using CAD and CAE software by comparing them with values obtained from experimental tensile destructive testing. This necessity arises from the absence of a universal testing machine in several educational centers unable to afford its acquisition cost, though they have access to such software. This approach aims to enhance the explanation of mechanical properties and improve the learning and understanding of students in technical fields. The document is structured as follows: Materials and Methods used, explaining the experimental test and the process to carry out the simulations. The results present the figures and values obtained for their respective analysis. The Discussion section compares the scope of the results with the information found in the literature, along with the authors' perspective. Finally, the Conclusions section synthesizes the most relevant information and presents the assertions derived from this research.

Materials and Methods

The shapes of tensile specimens can vary significantly, prompting the ASTM E8 standard (ASTM International, 2024) to define standard specimens for sheets,

thin sheets, tubes, jaws, and special specimen holders, along with standard round specimens for other metallic products. This standard specifies the initial lengths corresponding to all deformation values. Specimens must be manufactured without altering the material properties. The preferred specimen shapes, according to the ASTM E8 standard, are flat and round specimens, illustrated in Figure 1. This standard aims to outline the fundamental components of a tensile test and offers an overview of materials testing equipment, software, and necessary tensile samples. The dimensions provided by this standard have been consideredfor fabricating specimens in A36 structural steel.

Figure 1
Geometry of the specimen for the tensile test (ASTM International, 2024)

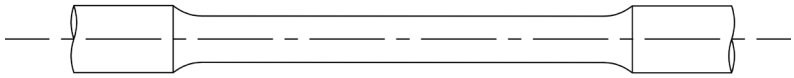

For the experimental tensile test, we utilized a Test Resources model 1608018 universal testing machine (Test Resources, 2024), which has a load capacity ranging from 15 to 150 kN. According to the manufacturer, it may have a minimum error of 0.2 % and a maximum value of 5 %, depending on the loads and clamping elements. A 12.7 mm diameter A36 structural steel shaft was machined following the dimensions specified in the ASTM E8 standard, as depicted in Figure 2a. Figure 2b illustrates the outcome of the tensile destructive test, where the specimen, as it undergoes permanent elongation, reduces its area until reaching the point of fracture. The maximum applied load was 34.53 kN, thus a value of 35 kN was designated for the application of the axial load in the simulations.

Figure 2
Specimen a) machined, b) after tensile test

In Figure 3a, the 3D modeling of the specimen conducted in CAD software, specifically SolidWorks, is depicted. This design was deemed essential to advance with the simulations. The process started with a structural static study within the CAD software. For the Finite Element Method (FEM) analysis, 10 861 elements and 47 060 nodes were generated for mesh creation, as illustrated in Figure 3b.

Figure 3
Specimen drawn in CAD software a) 3D modeling, b) meshing

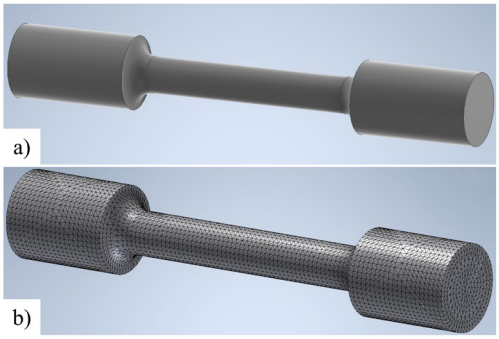

Figure 4a shows how a fixed support was placed on the cylindrical surface on the left side, where the specimen is attached to the base of the universal testing machine. Figure 4b illustrates the application of the axial load outward to the cross-sectional area of the specimen, which was defined as 35 kN, considering the maximum load value applied in the experimental test.

Figure 4
Initial conditions for the simulation a) fixed support, b) axial load

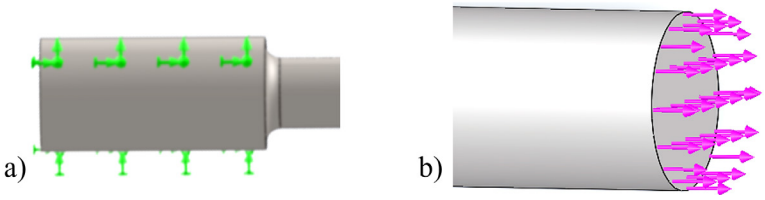

For the CAE analysis, we utilized the ANSYS software, equipped with various modules in the Workbench interface for conducting diverse studies. In Fig. 5a, it was noted that the mesh generation in the CAE software selected the default hexahedral option, resulting in 3 829 elements and 7 480 nodes. This meshing technique was continued due to its lower computational resource requirements, validated by the skewness metric, with an average value of 0.2403, considered excellent mesh quality as it falls below 0.25 (Simbaña et al., 2022). Fig. 5b provides an overview of the values achieved for discretizing the specimen in the mesh.

Figure 5
CAE Meshing: a) 3D Modeling, b) Metrics

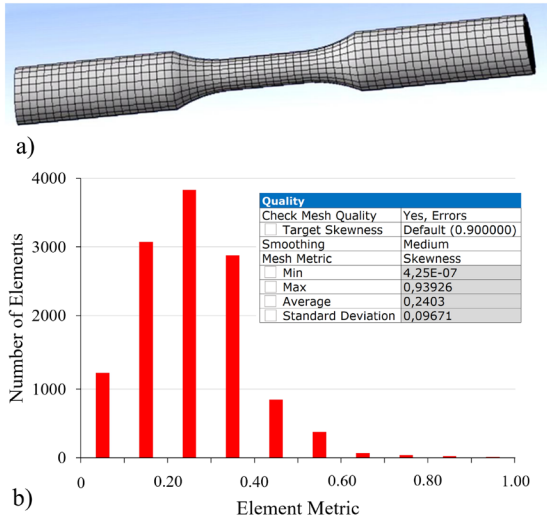

Results

Figure 6 illustrates the stress-strain curve derived from the specimens employed in the experimental tests. Specimen 1 attained the highest ultimate strength value at 434.8 MPa, while specimen 3 exhibited the lowest value for this stress at 415.8 MPa. The average ultimate strength obtained from these experimental tests was 422.45 MPa, accompanied by a mean deformation of 4.2 mm.

Figure 6
Stress-strain diagram of the specimens in the experimental process

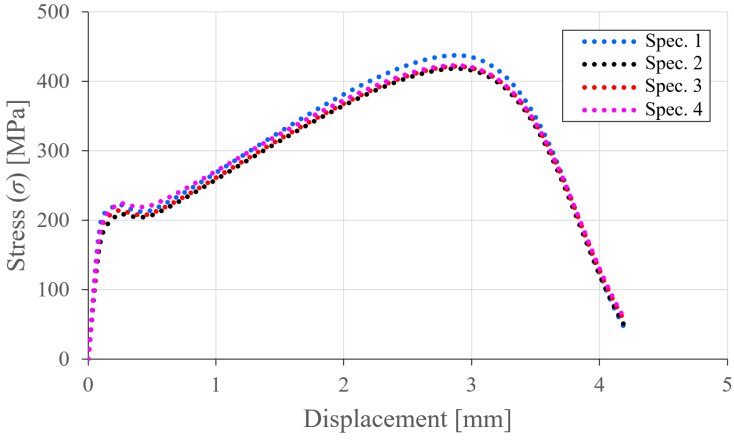

Figure 7 presents the outcomes of the computational numerical analysis for the tension test conducted in CAD software. It is noticeable that the most significant stress concentration appears in the regions where section changes occur, with the maximum stress recorded at 217.28 MPa. Although the color scale aids in comprehending the test results, the actual outcome, where the maximum stress ideally should be at the center of the specimen, is not distinctly evident. However, considering the dimensions recommended by the ASTM E8 standard and the application of the axial load obtained experimentally, the maximum stress closely aligns with the manufacturer's specified value of 420 MPa (American Metals Co., 2024).

Figure 7
CAD simulation for tensile stress

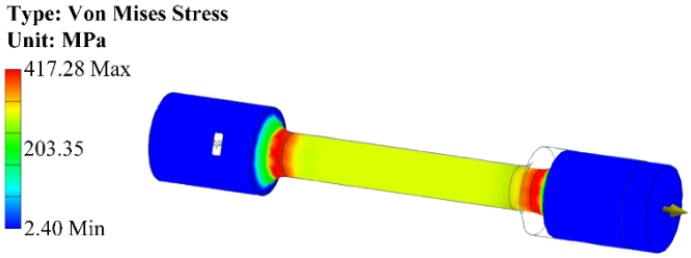

Figure 8 displays the outcomes of the simulation conducted with CAE, employing the Explicit Dynamics module of ANSYS software. The maximum stress achieved until the specimen ruptured was 426.59 MPa, under identical geometric conditions, constraints, and applied axial load.

Figure 8
CAE Simulation for Tensile Stress

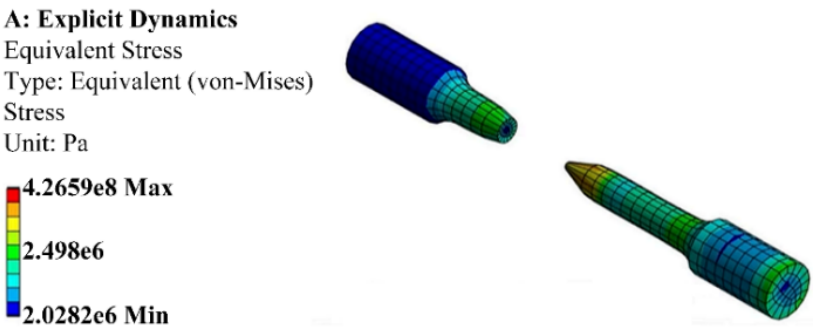

Figure 9 illustrates the stages obtained when conducting the simulation in specialized CAE software. This visually enhances the understanding of the process being conducted through the destructive tensile test, where the

application of axial load results in permanent elongation, leading to a reduction in the cross-sectional area until reaching the point where it cannot withstand the stress, ultimately leading to fracture.

Figure 9
Stages of CAE simulation for the tensile test

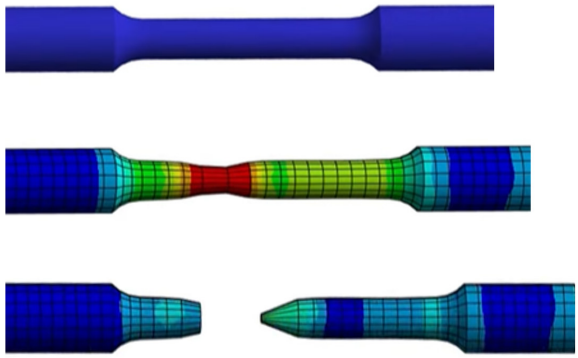

Figure 10 comparatively presents the stress values obtained for each procedure conducted in this research work, also indicating the stress value provided by the manufacturer of 420 MPa (American Metals Co., 2024). During the experimental destructive test, four specimens were used, and the average recorded stress was 422.45 MPa. On the other hand, through simulation in CAD and CAE software, the maximum stress was 417.2 and 426.59 MPa, respectively.

Figure 10
Comparative analysis of maximum stress results

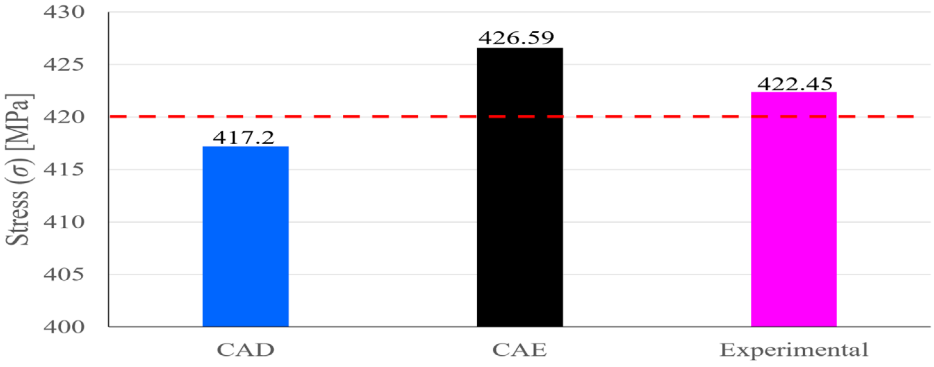

The accuracy of results produced by finite element methods relies on several factors, including the size of finite elements and the type of interpolation

functions employed. FEM models integrate mathematical equations with physical principles such as Newton's laws or Hooke's law, elucidating how forces interact with objects like polymer samples in test scenarios like compression or tension tests (Juárez-Luna and Ortiz Gálvez, 2021). Mesh generation procedures in software typically involve automatic meshing, which can be adjusted by concerning elements such as size, tolerance, and local control specifications. CAD or CAE software conceptualizes the model as a network of interconnected discrete elements. Meshing creates solid elements for individual analysis through discretization, with tetrahedra in 3D demonstrating the most reliable convergence (Ramírez et al., 2020). In the case of the tensile test, it starts with a theoretical phase, followed by sample preparation adhering to ASTM E8 standards [3], where cylindrical specimens with diameters of up to 12.7 mm are employed.

It is noteworthy that the manufacturer of A36 structural steel specifies in the datasheet that the maximum stress this material can withstand is 420 MPa. However, external factors exert an influence on this value, such as exposure to environmental conditions with abrupt temperature changes, rainfall leading to corrosion, and even mishandling, which may induce internal cracks, thus compromising the steel's quality. These factors contribute to the observed variability in the experimental maximum stress values, resulting in an average exceeding the manufacturer's specified value. Consequently, a relative error was calculated concerning the manufacturer's provided value for the three cases analyzed, amounting to 0.67, 1.56, and 0.56 % for the maximum stress obtained in CAD software, CAE, and experimental testing, respectively. In literature reviews, researchers like Serrano and Albán, (2022) have validated both experimental and numerical results when they fall within a 10 % difference. Therefore, it can be asserted that utilizing technological tools such as SolidWorks and ANSYS software is valid for conducting this tensile test via computational numerical analysis in scenarios where the necessary equipment is unavailable.

Conclusions

A comparative analysis was performed on the maximum stress values obtained in the tensile testing of A36 structural steel specimens, conducted through experimental destructive testing and utilizing CAD and CAE software. The literature review indicates that studies on the tensile properties of A36 structural steel primarily emphasize the welding process, predominantly comprising experimental studies. While studies employing FEM often focus on material composition enhancement, the objective of this research was to validate the simulation process in CAD and CAE software for the tensile test

as an alternative to the experimental approach, thereby contributing to the scientific domain.

In the destructive tensile test, we adhered to the ASTM E8 standard, employing a universal testing machine and four specimens. These specimens endured a maximum axial load of 34.53 kN, resulting in an average maximum stress of 422.45 MPa. SolidWorks as CAD software and ANSYS Explicit Dynamics module as CAE software were employed for physical discretization and subsequent computational FEM. The maximum stress values recorded were 417.2 and 426.59 MPa using CAD and CAE software, respectively. Comparing these with the manufacturer's specified maximum stress of 420 MPa for A36 structural steel, a relative error of 0.67 % was observed for CAD software and 1.56 % for CAE software, whereas for the experimental test, this error was 0.56 %. Hence, considering the dimensions outlined in the ASTM E8 standard and the configuration of the maximum axial load derived from experimental results, the maximum stress outcomes obtained through CAD and CAE software are deemed valid, contingent upon the proficiency and skills of individual users.

References

Alshoaibi, A. and Ali-Fageehi, Y. (2022). 3D modelling of fatigue crack growth and life predictions using ANSYS. Ain Shams Engineering Journal, 13(4), 101636. https://doi.org/10.1016/J.ASEJ.2021.11.005

American Metals Co. (2024). A36 Steel Technical Datasheet. https://www.metalshims.com/t-A36-Steel-Technical-Datasheet.aspx

Arroba, C., Flores, M.., Salinas, J., Ortega, S. and Ortega, H. (2021). Experimental Tests and Numerical Analysis of the Structure of the Alternative Composite Material for the Repair of Flight Surfaces in Aircraft. Enfoque UTE, 12(2), 37-51. https://doi.org/10.29019/ENFOQUEUTE.723

ASTM International. (2019). A36/A36M Standard Specification for Carbon Structural Steel. https://www.astm.org/a0036_a0036m-14.html

ASTM International. (2024). E8/E8M Standard Test Methods for Tension Testing of Metallic Materials. https://www.astm.org/e0008_e0008m-22.html

Barenghi, L., Barenghi, A., Cadeo, C. and Di Blasio, A. (2019). Innovation by Computer-Aided Design/Computer-Aided Manufacturing Technology: A Look at Infection Prevention in Dental Settings. BioMed Research International, 2019. https://doi.org/10.1155/2019/6092018

Berselli, G., Bilancia, P. and Luzi, L. (2020). Project-based Learning of Advanced CAD/CAE Tools in Engineering Education. International Journal on Interactive Design and Manufacturing, 14(3), 1071-1083. https://doi.org/10.1007/s12008-020-00687-4

Calderón, L., Bohórquez, O., Rojas, M. and Pertuz, A. (2021). Experimental Relationship of Tensile Strength and Hardness of Welded Structural Steel. Journal of Physics: Conference Series, 2046(1), 012065. https://doi.org/10.1088/1742-6596/2046/1/012065

Dhoska, K. (2019). Tensile Testing Analysis of the HRB400 Steel Reinforcement Bar. International Journal of Innovative Technology and Interdisciplinary Sciences, 2(3), 253-258. https://doi.org/10.15157/IJITIS.2019.2.3.253-258

Erazo-Arteaga, V. (2022). El diseño, la Manufactura y Análisis Asistido por Computadora (CAD/CAM/CAE) y Otras Técnicas de Fabricación Digital en el Desarrollo de Productos en América Latina. Información Tecnológica, 33(2), 297-308. https://doi.org/10.4067/S0718-07642022000200297

Fajardo, J., Villa, M., Pozo, J. and Urgilés, D. (2019). Characterization of the Tensile Properties of an Epoxy-Carbon Laminated Composite Used in the Development of a Single-seater Formula SAE Type. Enfoque UTE, 10(3), 1-12. https://doi.org/10.29019/ENFOQUE.V10N3.381

Falivene, L., Cao, Z., Petta, A., Serra, L., Poater, A., Oliva, R., Scarano, V. and Cavallo, L. (2019). Towards the Online Computer-aided Design of Catalytic Pockets. Nature Chemistry 2019 11:10, 11(10), 872-879. https://doi.org/10.1038/s41557-019-0319-5

García-Garrino, C., Careglio, C., Pacini, E., Miraso, A., Papeleux, L. and Ponthot, J. (2021). Procesamiento de Problemas de Mecánica de Sólidos en Entornos de Cloud Computing. XXIII Workshop de Investigadores En Ciencias de La Computación (WICC 2021, Chilecito, La Rioja), August 2021, 963-968. http://sedici.unlp.edu.ar/handle/10915/120382

González, O., Martínez, G. and Graciano, C. (2020). Evaluación Paramétrica de las Principales Variables Geométricas en el Diseño de un Tren de Aterrizaje para un Avión Notripulado Utilizando el Método de los Elementos Finitos. Revista UIS Ingenierías, 19(2), 149-160. https://doi.org/10.18273/REVUIN.V19N2-2020017

Gunter, S., Marchenko, E., Yasenchuk, Y., Baigonakova, G. and Volinsky, A. (2021). Portable Universal Tensile Testing Machine for Studying Mechanical Properties of Superelastic Biomaterials. Engineering Research Express, 3(4), 045055. https://doi.org/10.1088/2631-8695/AC41B4

Juárez-Luna, G. and Ortiz-Gálvez, P. (2021). Importancia del Mallado de Elementos Finitos de Muros de Mampostería Confinada en el Análisis Sísmico de Edificios. Revista Internacional de Ingeniería de Estructuras, 26(4), 712-745. https://doi.org/10.24133/RIIE.V26I4.2640

Larsen, I. L. and Thorstensen, R. T. (2020). The Influence of Steel Fibres on Compressive and Tensile Strength of Ultra High Performance Concrete: A Review. Construction and Building Materials, 256, 119459. https://doi.org/10.1016/J.CONBUILDMAT.2020.119459

Li, X., Zhang, Y., Shi, C. and Chen, X. (2020). Experimental and Numerical Study on Tensile Strength and Failure Pattern of High Performance Steel Fiber Reinforced Concrete Under Dynamic Splitting Tension. Construction and Building Materials, 259, 119796. https://doi.org/10.1016/J.CONBUILDMAT.2020.119796

Liao, W., Chen, P., Hung, C. and Wagh, S. (2020). An Innovative Test Method for Tensile Strength of Concrete by Applying the Strut-and-Tie Methodology. Materials 2020, Vol. 13, Page 2776, 13(12), 2776. https://doi.org/10.3390/MA13122776

Márquez-Herrera, A., Saldaña-Robles, A., Zapata-Torres, M., Reveles-Arredondo, J. and De la Peña (2022). Duplex Surface Treatment on ASTM A-36 Steel by Slide Burnishing and Powder Pack Boriding. Materials Today Communications, 31, 103703. https://doi.org/10.1016/J.MTCOMM.2022.103703

Prakash-Pasupulla, A., Abebe-Agisho, H., Seetharaman, S. and Vijayakumar, S. (2022). Characterization and Analysis of TIG Welded Stainless Steel 304 Alloy Plates Using Radiography and Destructive Testing Techniques. Materials Today: Proceedings, 51, 935-938. https://doi.org/10.1016/J.MATPR.2021.06.305

Rahangmetan, K. A., Wullur, C. W. and Sariman, F. (2020). Effect Variations and Types of Smaw Welding Electrodes on A36 Steel to Tensile Test. Journal of Physics: Conference Series, 1569(3), 032052. https://doi.org/10.1088/1742-6596/1569/3/032052

Ramírez, J. D., Cabezas, K., Jiménez, P., Canelos, R. and Escobar, B. (2020). Calculation of Voltage Distribution along the Insulator Strings of a 500 kV Transmission Line Based on Finite Element Method. Enfoque UTE, 11(3), 1-14. https://doi.org/10.29019/ENFOQUEUTE.V11N3.619

Ramos-Quintero, M., Campozano-Riofrio, R. and Naranjo-Vargas, E. (2022). Análisis y Simulación de Fuerzas en el Trabajo de una Prensa Hidráulica a Planchas de Acero de Distintos Espesores

Aplicadas en Perfiles Estructurales Angulares. Polo Del Conocimiento: Revista Científico - Profesional, 7(2), 1632-1655. https://doi.org/10.23857/pc.v7i2.3670

Rodríguez, M., Urday, E., Pantigoso-Gómez, E. and Andrade-Tacca, C. (2022). Evaluación de Propiedades Mecánicas de un Acero Estructural A-36 en la Formación de Ferritas. Revista Iberoamericana de Ingeniería Mecánica, ISSN 1137-2729, Vol. 26, No 2, 2022, Págs. 47-59, 26(2), 47-59. https://dialnet.unirioja.es/servlet/articulo?codigo=8996231&info=resumen&idioma=ENG

Serrano-Aguiar, C., Calispa-Aguilar, M., Ordoñez-Viñan, M., and Choto-Chariguamán, L. (2021). Efecto de Fisuras en la Tracción de Juntas Soldadas de Acero A36 Mediante Simulación Numérica. Conciencia Digital, 4(4.2), 77-100. https://doi.org/10.33262/concienciadigital.v4i4.2.1948

Serrano, C. and Alban, D. (2022). Evaluation of Mechanical Properties and Metallographic Characterization of ASTM A36 Steel Welded Joints Under the GMAW Process. 1303-5150. https://doi.org/10.48047/nq.2022.20.22.NQ10250

Simbaña, I., Quitiaquez, W., Estupiñán, J., Toapanta-Ramos, F. and Ramírez, L. (2022). Performance Evaluation of a Direct Expansion Solar-assisted Heat Pump by Numerical Simulation of the Throttling Process in the Expansion Device. Revista Técnica "Energía," 19(1), 110-119. https://doi.org/10.37116/REVISTAENERGIA.V19.N1.2022.524

Test Resources. (2024). 315 Universal Test Machines. https://www.testresources.net/test-machines/universal-testing-machines/300-series/315

Vantyghem, G., De Corte, W., Shakour, E. and Amir, O. (2020). 3D Printing of a Post-tensioned Concrete Girder Designed by Topology Optimization. Automation in Construction, 112, 103084. https://doi.org/10.1016/J.AUTCON.2020.103084

Wei, W., Peng, F., Li, Y., Chen, B., Xu, Y. and Wei, Y. (2021). Optimization Design of Extrusion Roller of RP1814 Roller Press Based on ANSYS Workbench. Applied Sciences 2021, Vol. 11, Page 9584, 11(20), 9584. https://doi.org/10.3390/APP11209584

Zhou, T., McBride, K., Linke, S., Song, Z. and Sundmacher, K. (2020). Computer-aided solvent selection and design for efficient chemical processes. Current Opinion in Chemical Engineering, 27, 35-44. https://doi.org/10.1016/J.COCHE.2019.10.007